Supporting Information

Prather *et al.* 10.1073/pnas.0806541106

SI Text

As part of this comparison between 2 chemistry-transport models (CTMs), the University of California, Irvine (UCI) CTM identified weaknesses in the tracer transport code. The resulting changes in the SOM algorithms have increased the accuracy, improved the parallelization, and greatly reduced the computational time. These and previous developments since Prather *et al.* (1) are likely to have general application to many CTMs and are described briefly here.

New SOM Flux Limiters and Associated Errors. A critical component of high-order advection algorithms is the method of fitting the distribution of tracer abundance used to calculate the amount of tracer transported with the winds. In the SOM algorithm, the fit to the tracer abundance (i.e., mass mixing ratio) is always with the 9 second-order moments: x, x^2, y, y^2, z, z^2, xy, yz, zx. Without limiters, the transport of a square-wave (i.e., abundance 100 on a background of zero as shown in Fig. S1) conserves mass, but the moments predict a region of negative tracer in advance of the leading edge and also following the trailing edge. This is shown for the zero limiter case Lim = 0 (green dotted lines in Fig. S1). We have never used Lim = 0 in scientific studies because negative tracer amounts appear in subsequent advective steps. The SOM is made positive-definite with Lim = 1 that adjusts the moments along the direction of transport (e.g., only the x and x^2 moments for U transport) to maintain a positive parabola (blue solid line in Fig. S1). This limiter was the original choice for most CTM simulations. Since Prather *et al.* (1), the problems with unphysical, numerical induced ripples in the tracer abundance led to introduction of Lim = 2, which forced a monotonic tracer abundance within a grid box (red dotted line). The limiter Lim = 3 (magenta solid line) introduced a min–max criteria whereby the 1D moments were additionally reduced to ensure that the min–max of tracer abundance in the daughter box was constrained by the min–max of the 2 parent boxes. All of these limiters operate in 1 dimension along the transport direction (e.g., x and x^2 for U transport), but it is not obvious how to control the cross-moments (e.g., xy and zx). In the current code, these cross moments are limited by ± 1 times the amount of tracer mass in the box (see code in Dataset S1).

Both LR and SOM are flux-based algorithms in which the tracer abundance in a rectilinear grid box is changed by the flux of tracer and air mass across the 6 boundaries. In contrast to the SOM algorithm, the LR algorithm does not store and then maintain the moments during transport, but at the start of each advection step LR generates polynomial expressions for the tracer abundance (similar to the SOM moments) step based on the 3D distribution of the mean tracer abundance in neighboring grid boxes. The LR algorithm in the GMI CTM also reverts to a different, semi-Lagrangian algorithm at high latitudes to avoid violating the CFL criterion. It further averages the tracer abundance over the polar cap and adjacent latitude ring. The LR algorithm requires that the polar cap have exactly half the latitude extent of all of the other grid boxes, and thus it is impossible to simply embed a doubled resolution grid. The original SOM algorithm had similar problems at the poles, but these have been corrected with the new algorithm (see below). The SOM algorithm has no requirements on uniformity of size/mass of the grid boxes.

To examine the type of errors expected with SOM, we calculate 3D advection of a cube with uniform tracer in a zero background. With uniform flow, this is a much simpler test than the realistic, time-varying, divergent flow of the real atmosphere, but it is important to do such tests in 3D because errors in 1D and 2D are deceptively less. The flow is taken as uniform but cutting across the grid: $U = 1/8$, $V = 1/8$, $W = 1/4$. The errors for a $6 \times 6 \times 6$ cube are given in Table S1. The minimum and maximum of tracer over the entire domain show the unphysical ripples typical of high-order advection algorithms. SOM Lim = 0 imposes no constraints on the 9 moments, has modest overshoot (8%) and undershoot (−11%), but is the most accurate in terms of maximum absolute error or rms error. Typical of high-order methods, the rms error rises quickly to 27% after 10 grid steps, but then increases more slowly (e.g., 45% after 100 grid steps) as the method establishes the shape that it prefers to advect. This pattern is seen in both max and rms error for all limiters. SOM Lim = 1 forces positive definite tracer and hence there is no undershoot, but at the price of greater overshoot (11%). SOM Lim = 2 adds monotonicity that reduces the overshoot (9%) but again increases the error. The min–max Lim = 3 eliminates most overshoot/undershoot but eventually becomes more diffusive (i.e., by grid step 100 the maximum in the cube drops to 78%).

Improvements that reduce unphysical ripples increase the error. Errors increase monotonically with stringency of flux limiters from Lim-0 to Lim = 3, but the relative increase is modest, a factor of 1.5 at most, and likely worth the price to avoid unphysical ripples in the tracer distribution. Although not apparent in the table, SOM Lim = 3 generates small overshoots at the 1% level in these tests because the cross-moments are difficult to constrain without adding too much diffusion. In 2D flow the Lim = 3 overshoots are $<0.04\%$, and there are absolutely none in 1D flow. In evaluating unphysical ripples in any advection method, 3D tests are essential.

3D Operator Split as 1D Pipe Flow. The 3D transport of tracers is calculated in the UCI CTM as 3 sequential 1D pipe flows as shown in Fig. S2 *A* and *B*. The 3D information on the tracer distribution is contained in the cross-moments, so that advection in any direction can be calculated as 1D pipe flow. The E–W flow on a globe is naturally cyclic with grid box N connecting to box 1. The new N–S flow is over the pole and connects 2 opposite meridians into a ring (see Fig. S2*A*). Vertical advection can be treated as cyclic by connecting the model top to bottom with a zero-flux boundary (see Fig. S2*B*).

The 1D pipe flow (calculated in subroutine QVECT3, given in Dataset S1) has been vectorized through the adoption of a sequential odd–even calculation of transport across boundaries (Fig. 2*C*). This approach eliminates the dependencies in previous SOM algorithms (e.g., transport between boxes 2 and 3 awaits completion of transport between boxes 1 and 2), but changes the order of calculation and thus does not preserve the bit-level comparison with previous versions. The single subroutine QVECT3 handles U, V and W advection through the formal parameters and is a notable improvement over the 3 separate subroutines in ref. 2.

Over-the-Pole Flow. Advective transport over the pole on a regular latitude × longitude grid is prone to large error. A basic problem, as shown in Fig. S3, is that low-Courant number N–S advection becomes high-Courant number E–W flow at the pole and is then reversed. The SOM algorithm with cross-moment readily handles this shift from N–S to E–W. True polar flow also requires transport across the apex of pie-shaped boxes at the polar cap.

We develop a new algorithm for transport at 90° latitude as shown in Fig. S4.

The new algorithm connects meridians on opposite sides of the pole into a 360° cyclic meridional ring, similar to that for longitudinal transport. For the meridian on the "opposite" side, the V winds and all first-order y-moments (y, xy, yz) reverse sign. The 2 pie-shaped polar boxes are combined conserving all tracer moments. After transport the north and south boxes at the pole are divided into 2 equal air masses and placed back on the original grid. The tracer mass in each of the split boxes is not equal but determined by the moments. If the polar box and its opposite partner have excess air mass then an E–W U field is generated, flowing outward from both sides and reaching halfway around the polar cap. This U field redistributes the excess air mass uniformly across all polar boxes. The U fields from all polar box pairs are summed, and a single E–W advective step is calculated. Thus the polar U fields are not taken directly from the meteorology but from the divergence of the V fields into the polar cap. This polar redistribution of air mass results in a uniform W field across the polar cap.

Results from this new over-the-pole advection are compared with those from the 1987 CTM in Fig. S5. For a solid-body rotation angle of 30°, the transport of an equatorial 6×6 block of tracer once around the sphere is unchanged by the new polar treatment. The results from new and old SOM algorithms are very close, but differ slightly because of the new odd–even pipe flow. For angles of 80° and 90° the improvement is clear: The transported block maintains its quasirectangular appearance and has little more diffusion than for a rotation at a 30° angle.

CFL and Lipschitz Criteria—Upper Limits on Time Steps. The current SOM formulation has a maximum time step limited by the Courant–Freidrich–Levy (CFL) criterion that the air mass flux cannot remove more mass than is contained in the box. An alternative SOM pipe flow algorithm may get around this by moving the boundaries of the boxes downstream (across several existing grid boxes) and then consolidating the boxes or fractions between the new boundaries. We chose instead to implement the 1D pipe flow as described above, but implement the CFL criterion as needed for each individual pipe. The subroutine QVECT3 analyzes the flow field, determines the maximum time step based on the CFL criterion, and then performs a multiple number of smaller time steps. This multistepping is internal to QVECT3 and extremely fast because the transport calculation is repeated on locally stored variables. A similar approach for the U fields at high latitudes was invoked by Russell and Lerner (3) to increase the global CFL time step.

The inclusion of an autoCFL criterion that is local to each 1D pipe means that only the Lipschitz criterion (e.g., ref. 4) constrains the global time step. In our case the Lipschitz criterion can be expressed as a divergence criterion: For a given time step, the mass in any grid box during the operator-split advection sequence must not reach zero. For each 3-hour averaged wind field, a maximum time step is computed for the current $W + V + U$ sequence of mass fluxes, and if it is less than the requested operator-split time step then an integral number of substeps is set for the global calculation. Our wind fields are generated as 3-hour averages, and the CTM maintains constant U, V, and W fluxes over the 3 hours.

The combination of an autoCFL in each pipe combined with the global Lipschitz criterion greatly reduces the cost of advecting tracers compared to a global CFL criterion. This advantage is necessary as we move to $1° \times 1°$ resolution but still wish to retain an operator-split time step of ½ to 1 h based on the time scales for photochemistry, convection, and boundary layer mixing.

Operator Splitting and Parallelization. The CTM calculation sequence for processes that alter the tracer distribution has evolved to minimize the amount of computation and take advantage of OpenMP parallelization. It is outlined in Dataset S2. We have split the parallel task for individual CPUs into (*i*) blocks covering a range of latitudes and longitudes with all levels to compute emissions, photochemistry and all vertical transport across all tracers and (*ii*) single layers globally to compute U and V transport for all tracers.

The operator-split time step is set by the desired frequency of diagnostics and a recognition of the inherent time scales of the problem (e.g., photochemical change during sunrise). The operator-split time is further subdivided if the Lipschitz criterion is not met. The order of operators will change the diagnosed tracer abundances.

Convection has been modeled as 2 steps: Convective updrafts, downdrafts, and detrainment, followed by redistribution back to the original air mass in each layer with a with a vertical wind field W_C. We combine W_C with the large-scale wind W that is calculated from the convergence of U and V and do a single W advection step. In the tropics, much of the boundary-layer convergence can be carried aloft in convective plumes, and thus primary effect of subsidence (Wc) is to cancel this convergence-driven large-scale vertical wind (W). Some researchers have argued that combining W_C plus W is necessary to eliminate redundant transport and reduce the numerical diffusion, but with SOM the primary advantage is in computational savings.

1. Prather M, McElroy M, Wofsy S, Russell G, Rind D (1987) Chemistry of the global troposphere: Fluorocarbons as tracers of air motion. *J Geophys Res* 92:6579–6613.
2. Prather MJ (1986) Numerical advection by conservation of second-order moments. *J Geophys Res* 91:6671–6681.
3. Russell GL, Lerner JA (1981) A new finite-differencing scheme for tracer transport equation. *J Appl Meteorol* 20:1483–1498.
4. Tanguay M, Polavarapu S (1999) The adjoint of the semi-Lagrangian treatment of the passive tracer equation. *Mon Weather Rev* 127:551–564.

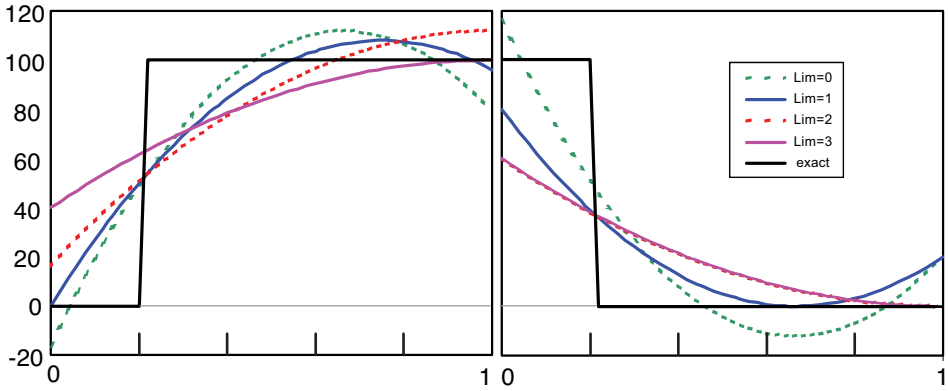

Fig. S1. SOM transport of a 1-box step-function from left to right with a single Courant step of 0.2. The exact answer is the square-wave displaced (solid black line) and the colored curved lines show the inferred distribution of tracer within each grid box using the second-order moments with limiters Lim = 0 (green dashed line, no limits, goes negative), Lim = 1 (blue solid line, positive definite), Lim = 2 (red dashed line, monotonic), and Lim = 3 (magenta dashed line, bounded by min/max of parent boxes). The total amount (zeroth moment) in each case is exactly the same (left 80, right 20).

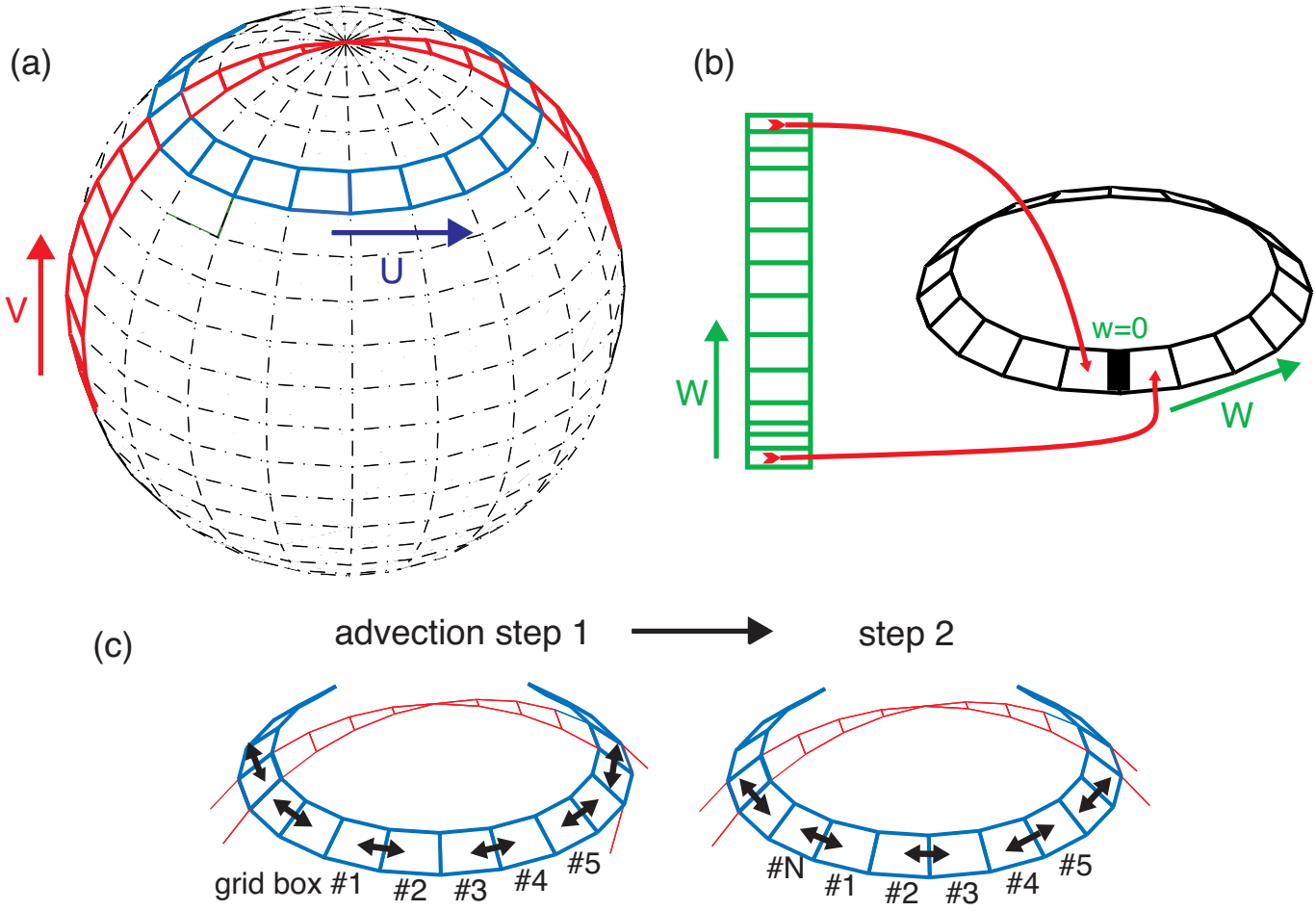

Fig. S2. Decomposition of 3D tracer advection into 1D vectorized pipe flows. (*a* and *b*) Schematic of the new SOM piped flow for *U* and *V* advection (*a*) and *W* advection (*b*). All 3 directions are treated as a cyclic, piped flow. For E–W transport (*U*) this is obvious, for N–S transport (*V*) this requires over-the-pole flow that connects opposite meridians; and for vertical transport (*W*) it requires an artificial connection between top and bottom layers with zero air mass flux. (*c*) Calculation sequence for *U* advection. The new vectorized algorithm avoids the dependencies of the original SOM algorithm by calculating advection between even pair of boxes (step 1: 1–2, 3–4, 4–5, …) as a vector operation and then between odd pairs (step 2: N−1, 2–3, 4–5, …). N must be even.

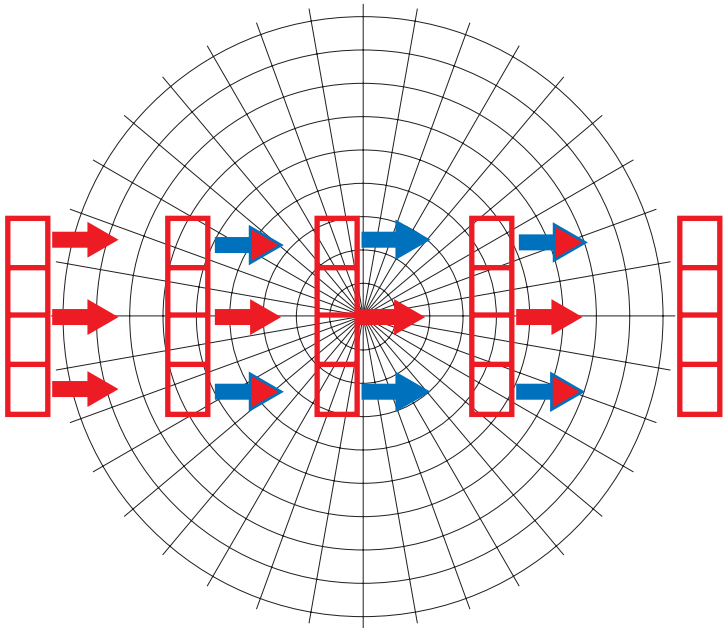

Fig. S3. Schematic for over-the-pole flow of four equatorial boxes, showing how N–S advection must be converted into high-Courant number E–W flow at the pole and then reversed.

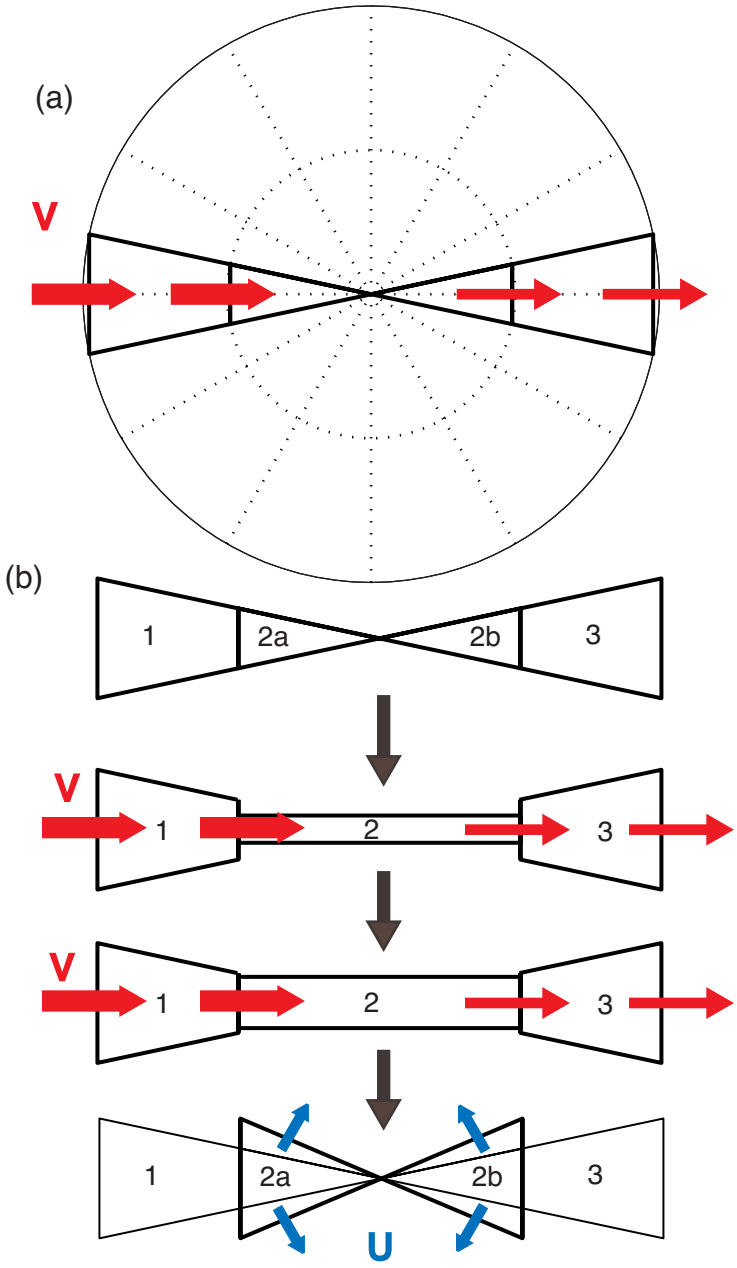

Fig. S4. Schematic of over-the-pole advection. (*a*) North–south transport couples meridians on opposite sides of the globe. (*b*) Boxes 1, 2a, 2b, and 3 become part of a 1D pipe flow. All first-order *y*-moments in 2b and 3 reverse sign. Boxes 2a and 2b are combined, preserving all 9 moments. 1D pipe flow is computed for the entire meridional (*V*) circle, including the over-the-pole sequence 1–2-3. After advection, box 2 is split equally in air mass, using the moments to partition tracer and its moments into boxes 2a and 2b. In the example, the air masses in these boxes are larger than expected and thus induce an east–west (*U*) transport in the polar cap that reaches halfway around, equally distributing the excess air mass.

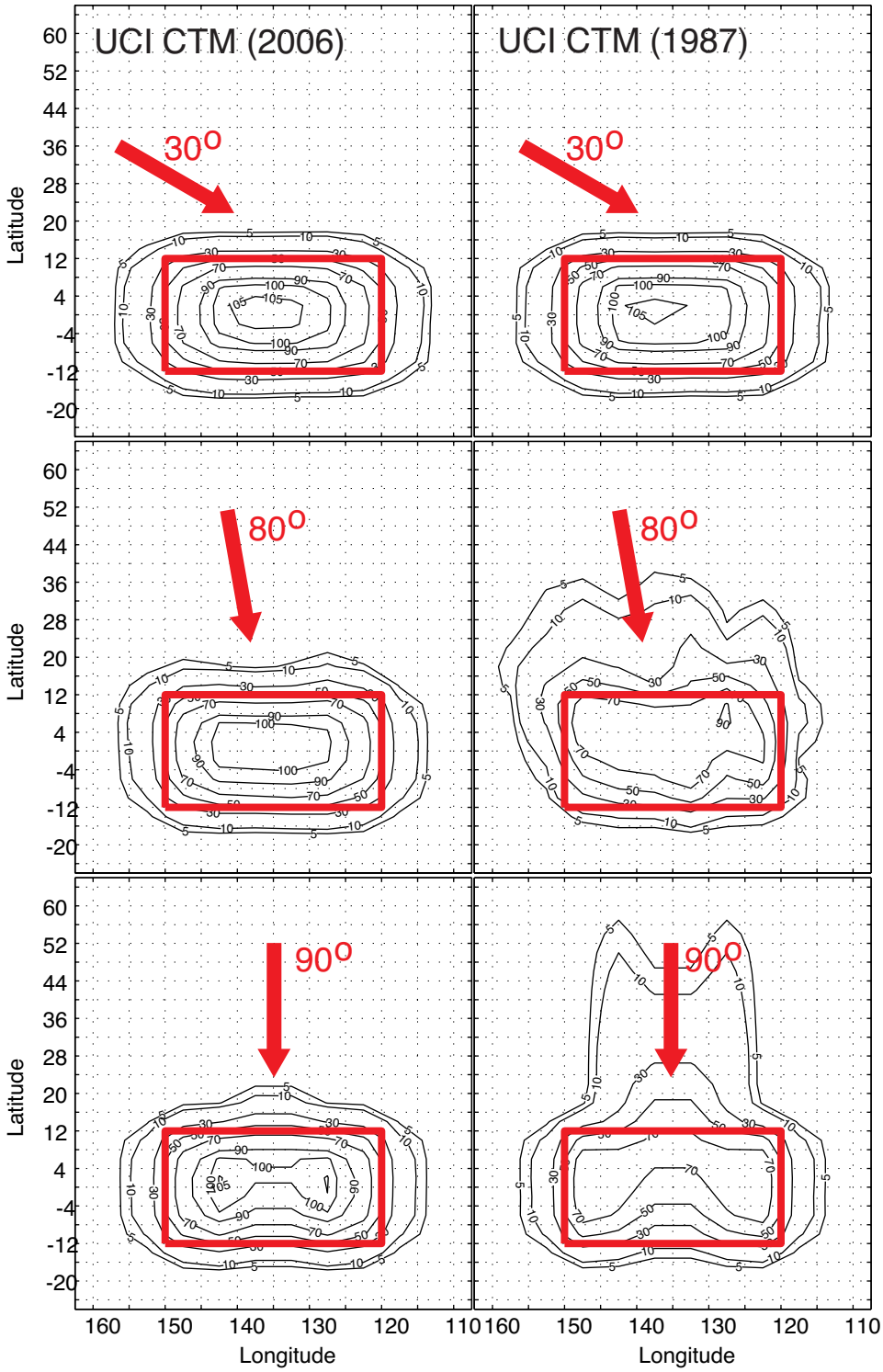

Fig. S5. Advection of a 6 × 6 equatorial block over the pole with solid-body rotation. The original block (square outlined with thick red line) has tracer units 100 on a zero background. Results after a 360° rotation are shown with black contour intervals of 5, 10, 30, 50, 70, 90, 100, and 105. SOM Lim = 2 is used with the new 2006 code (*Left*) and the original CTM formulation (*Right*) (1). The 1987 CTM averaged the tracer over the entire polar cap. The 2006 CTM uses the algorithm shown in Fig. S4. The direction of solid-body rotation is shown by the red arrows and labeled by the tilt as 30°, 80°, and 90°.

Table S1. Advection errors for different SOM limiters

Lim	Grid step	Min	Max	Max|err|	rms err
0	10	−8	108	49	27
	30	−10	108	59	36
	100	−11	104	68	45
1	10	0	111	58	30
	30	0	109	67	38
	100	0	110	77	48
2	10	0	106	60	33
	30	0	109	68	39
	100	0	107	76	48
3	10	0	100	65	40
	30	0	98	71	48
	100	0	78	75	57

A $6 \times 6 \times 6$ block with tracer abundance = 100 is advected in an effectively infinite zero background. The operator split sequence is U–V–W–V–U with W = 1/4 and $U = V$ = 1/8. For SOM Lim = 0–3, the error growth is shown as the number grid steps increases to 100 (4 operator split steps = 1 grid step). The minimum/maximum of the tracer show the undershoot/overshoot in each limiter. The maximum absolute error and rms error are calculated over the entire domain. The sum of the square of the errors is divided by 216 before taking the square root.

Other Supporting Information Files

Dataset S1 (TXT)
Dataset S2 (PDF)